Open access • Journal Article • DOI:10.1007/BF01407827

Particle Production in Hadron-Nucleus Collisions in a Multi-Chain Fragmentation Model — Source link

J. Ranft, S. Ritter

Institutions: CERN, Leipzig University

Published on: 27 Apr 1983 - European Physical Journal C (Springer-Verlag)

Topics: Hadron, Baryon and Meson

EUROPEAN ORGANIZATION FOR NUCLEAR RESEARCH

[redacted]

TIS-RP/103/PP

27 avril 1983

PARTICLE PRODUCTION IN HADRON-NUCLEUS COLLISIONS IN A MULTI-CHAIN FRAGMENTATION MODEL

J. Ranft*)
CERN, Geneva, Switzerland

S. Ritter
Karl-Marx-Universität, Sektion Physik, Leipzig, DDR

ABSTRACT

We investigate a multi-chain fragmentation model for particle production in hadron-hadron and hadron-nucleus collisions for all kinds of incident hadrons. The model is implemented using a realistic Monte Carlo model for the fragmentation of quark-antiquark, quark-diquark, and diquark-antidiquark chains into mesons, baryons, and their resonances. We assume that these jets have universal properties which are the same in electron-positron, lepton-hadron, and hadron-hadron collisions. Energy-momentum and all additive quantum numbers are exactly conserved. The model is compared with exclusive as well as inclusive particle-production cross-sections. It is well suited to the study of complete exclusive events and the flavour composition of secondary multiparticle systems.

(Submitted to Z. Phys. C)

*) Present address: Karl-Marx-Universität, Sektion Physik, Leipzig, DDR.

1. INTRODUCTION

Multihadron production in soft hadron-hadron and hadron-nucleus collisions is one of the fields where serious predictions from quantum chromodynamics (QCD) are missing. These processes are dominated by unperturbative properties of QDC. Nevertheless, during the last 10 years in this field we have seen a complete change of the basis of the models which are used to interpret the data. From Regge-type and statistical models we have moved to models constructed in the framework of the parton model. To describe hadronic multiparticle production, the parton model is used together with dynamical assumptions introduced on purely phenomenological grounds. The hope is that these dynamical assumptions will eventually be demonstrated in QCD. At present it is not even clear whether the partons used in soft multihadron production models are the same objects that occur in hard processes described by perturbative QCD.

The two most important types of models for particle production in hadron-hadron collisions are recombination models and fragmentation models. Quark recombination models [1] start from the observation [2] that parton distributions in deep inelastic scattering and secondary-hadron x-distributions in hadron-hadron collisions are rather similar. Fragementation models were first studied by the Lund group [3]. The origin of these models is the similarity of the Feynman x-distributions of hadrons in hadronic collisions to parton fragmentation functions. In Ref. [3] the underlying dynamical model is the picture of chromoelectric flux-tube breaking via $q\bar{q}$ pair creation. Most other applications of the fragmentation model [4] start from the dual topological unitarization (DTU) scheme (see Capella [5] for a review). This is the approach which we will follow also in our model.

So far both, recombination and fragmentation, models seem to describe all essential features of the data.

Particle-production processes in hadron-nucleus collisions involve one additional feature, which cannot be studied in hadron-hadron collisions. This is the space-time evolution of the scattering process [6]. One of the outstanding features of particle production in high-energy hadron-nucleus collisions is the absence of intranuclear cascading of fast secondaries. The favoured interpretation of this fact is that the fast secondaries are created outside the nucleus.

Faessler [7] gave a recent experimental review of the main features of particle production in high-energy hadron-nucleus collisions. Two of the most popular theoretical models to describe hadron production in h-A collisions are the constituent quark model [8] and the DTU-based fragmentation models. In the latter models, the approach used by the Austin group [9] differs from that of the Orsay group [10]. We will follow here the scheme of Capella and Tran Thanh Van [10].

The aim of our paper is the following. We want to construct a model which reproduces correctly the projectile dependence in hadron-hadron collisions and the A-dependence in hadron-nucleus collisions. Especially, we are interested in creating exclusive events which fulfil all requirements of quantum-number and energy-momentum conservation. This will allow us to study all kinds of exclusive features and correlations. So far [4,5,10] the fragmentation models were mainly used to study inclusive cross-sections. Our model should also describe the production of all kinds of secondary mesons and baryons as well as hadron resonances. The property which allows us to fulfil all these requirements is "jet universality". As reviewed by Kittel [11], particle production in soft hadronic collisions shows features very similar to quark-antiquark jets in e^+e^- and diquark jets in lepton-hadron collisions. We use a realistic model for the fragmentation of quark and diquark jets into the observed hadrons.

In the present work we apply an extended version of a Monte Carlo chain-decay model developed earlier by us [12], which has been carefully tested in a comparison with quark-antiquark two-jet events produced in e^+e^- annihilation [12,13]. The extended version of this model used here [14] simulates, besides the hadronization of quark-antiquark two-jet systems, also the transition of (anti)quark-(anti)diquark and diquark-antidiquark two-jet systems into hadrons. The conservation of energy-momentum and quantum numbers for such two-jets is always guaranteed. For testing the model of diquark fragmentation into hadrons one can use data from lepton-hadron interactions [15]. In order to apply this Monte Carlo chain-decay model also to hadron-hadron collisions, the basic assumption we have to make is that quark and antiquark jets produced in e^+e^- annihilation and diquark jets from deep inelastic lepton-hadron collisions should not differ strongly from those produced in hadron-hadron collisions.

The version of the model as described here and our comparison with experiment is still limited. Here we are only interested in the particle production at moderate energies, say for 5 to 10 GeV up to around 1 TeV. Therefore it is sufficient to consider just two chains involving only valence quarks in hadron-hadron collisions. In order to describe the particle production at the energies of the CERN SPS proton-antiproton collider we have to add [16] further chains involving also sea quarks according to the AGK rules [17]. Such an extension of the model [16] seems to describe those features of particle production known at present at these energies; see also Refs. [18]. In this paper we shall not study in detail such problems as the production of leading particles, two-particle correlations, charge correlations, threshold effects at small energies, and the inclusion of diffractive particle production.

The contents of this paper are as follows. In Section 2 we give a short summary of the multi-chain model used for hadron-hadron and hadron-nucleus interactions and in Section 3 we discuss our chain-decay fragmentation model. The formulation of the whole model via a Monte Carlo method is described in Section 4. In Section 5 we present results of the model and compare it with data.

2. THE MULTI-CHAIN MODEL FOR HADRON-NUCLEUS COLLISIONS

Capella and Tran Thanh Van developed the two-chain model for hadron-hadron interactions [4] on the basis of the DTU scheme. They further generalized it to a multi-chain model for hadron-nucleus interactions [10]. In the following we refer to these models.

In hadron-scattering processes we assume that the interaction separates the valence quarks in each incident hadron into two coloured systems. For an incident proton we obtain a quark and a diquark sharing the proton momentum. The interaction gives rise to two multiparticle chains. In this simple version the chains are built up only from the valence quarks of the interacting hadrons. In Fig. 1a, b, and c we show all possible two-chains for baryon-baryon, antibaryon-baryon, and meson-baryon interactions. The energy or momentum fraction x carried by the single valence quarks contributing to a chain is obtained using valence quark distributions. In the case of baryons the dressed diquark now gets the remaining energy $1-x$. Using such a scheme the dressed diquarks carry in general larger x fractions than the single valence quarks. In the case of mesons we have two possibilities. Either we sample at first the x-fraction of the valence quark and give the valence antiquark the remaining energy $1-x$ or vice versa. The invariant masses of the chains are now completely defined by the x fractions and the c.m. energy of the collision.

As already discussed in the Introduction, building up the chains only from valence quarks is not correct for larger energies, i.e. at collider energies.

In the case of hadron-nucleus scattering the model becomes more complicated since many interactions may occur. The average number of collisions, $\bar{\nu}$, inside the nucleus is given by the mass number A and the inelastic cross-sections for hadron-hadron and hadron-nucleus interactions:

$$\bar{\nu} = A\sigma^{h-h}_{inel}/\sigma^{h-A}_{inel} \, . \qquad (1)$$

Each collision provides two chains as in a hadron-hadron interaction. So we get finally two $\bar{\nu}$ chains on the average. In Fig. 2 we show an example for a simple triple-scattering process in a proton-nucleus collision. As is seen from Fig. 2, both the valence quarks and the sea quarks of the projectile have to be included to construct the chains. Two chains are initiated by the valence quarks of the projectile and the valence quarks of the target nucleons. All other chains are derived from sea quarks of the projectile and valence quarks of target nucleons.

3. THE CHAIN-DECAY FRAGMENTATION MODEL

The chain-decay model for the fragmentation of quark and diquark jets used here is based on an earlier version of this model [12,13], which was tested using data from e^+e^- annihilation. We have now extended the model to produce complete quark-antiquark two-jets as well as (anti)quark-(anti)diquark and diquark-antidiquark two-jet systems [14] with arbitrary initial quark flavours (u,d,s, or c quarks). In Fig. 3a and b we show typical two-jet systems produced by an initial quark and diquark or an initial diquark and antidiquark.

The fragmentation of diquarks into mesons and baryons can be tested using data from lepton-hadron interactions [15].

A detailed description of this chain-decay model as well as of the underlying Monte Carlo formulation is given in Refs. [12,13,14]. Here we want to discuss only some basic features of the model:

i) In the case of complete two-jet systems the model guarantees exact energy-momentum and quantum-number conservation.

ii) The model includes the fragmentation of quarks and of diquarks into mesons as well as into baryons. All possible vertices during the chain decay of an initial (anti)quark or (anti)diquark and the corresponding probabilities are given in Fig. 4.

iii) The quark flavours at each actual vertex during the chain decay are sampled according to a quark-mass-dependent distribution [12], which provides in our case approximately the following probabilities of creating a $u\bar{u}$, $d\bar{d}$, or $s\bar{s}$ pair: $P_{u\bar{u}} = P_{d\bar{d}} \approx 5P_{s\bar{s}}$. An an extension to the model described in Ref. [12] we have also included isospin conservation for incoming u or d ($\bar{u}$ or $\bar{d}$) quarks. This provides for an incoming $u(\bar{u})$ quark $P_{d\bar{d}} = 2P_{u\bar{u}}$ and for an incoming $d(\bar{d})$ quark $P_{u\bar{u}} = 2P_{d\bar{d}}$.

iv) At each vertex the emitted hadron carries an energy fraction z from the incoming parton and leaves behind a parton jet carrying the energy fraction $1-z$. In order to describe leading baryon effects one should choose a much flatter energy-sharing function f(z) in the case of incoming diquarks forming baryons

$$f(z) = \text{const.} \quad (2)$$

than in all other cases, where

$$f(z) = 1 - a + 3a(1-z) , \qquad a = 0.88 . \quad (3)$$

v) Our model has no freedom concerning the flavour contents of the jets. Determining the flavours of the initial partons of the chain, the flavour contents of the final hadron two-jet is defined by the model and quantum-number conservation.

vi) The mentioned two-jet systems can be considered as colour neutral objects. This simplifies the model for hadron-nucleus collisions, where many two-chains are produced.

vii) The decay of quarks and diquarks into hadrons is realized via pseudoscalar and vector mesons and baryons with spin $\frac{1}{2}$ and $\frac{3}{2}$, respectively.

viii) For most applications we consider the decay of hadron resonances into final stable particles using the Monte Carlo code DECAY [19].

4. FORMULATION OF THE MODEL VIA A MONTE-CARLO METHOD

In Section 2 we have discussed the multi-chain model for hadron-nucleus interactions on the parton level and in Section 3 we gave a short summary of our hadronization scheme. Now we describe the formulation of the whole model via a Monte Carlo method. For simplicity we first discuss the event generation in hadron-hadron interactions. It proceeds by the following steps:

1) Define the kind of projectile P and target T, i.e. the valence-quark constituents of these particles, and the laboratory momentum p_0 of the projectile.

2) Make a Lorentz boost into the c.m.s. of the projectile and the target particle.

3) Decide what kind of chains have to be constructed depending on the projectile and the target particle (see Fig. 1a-c). For meson-baryon collisions we have two possibilities: the quark or the antiquark of the meson may belong to the forward chain, i.e. carry the larger momentum fraction x of the meson.

4) Select initial flavours of the considered chains using only the valence quarks of the projectile and target.

5) Sample the energy or momentum fraction x of the single valence quarks according to the distribution

$$d_B^{val}(x) \sim \frac{(1-x)^{5/2}}{x^{1/2}} \tag{4}$$

for baryons and according to

$$d_M^{val}(x) \sim \frac{(1-x)^{1/2}}{x^{1/2}} \tag{5}$$

for mesons. The diquarks of the projectile or target are given the remaining energy 1 - x. The invariant masses of the chains are now well defined by the x-fractions of the initial partons and the c.m. energy of the collision.

6) Now we have to hadronize the two-jet systems on the basis of the Monte Carlo chain-decay model characterized in Section 3. Of course this is only possible if the invariant masses of the chains are large enough. We proceed in the following way:

i) For $M_{chain} \geq m_{H^*} + 300$ MeV/c^2 the chain decay occurs, where m_{H^*} is the mass of the hadron resonance defined by the initial quarks of the chain (vector meson or spin 3/2 baryon).

ii) For $m_{H^*} \leq M_{chain} \leq m_{H^*} + 300$ MeV/c^2 we correct the momentum fractions x of the initial quarks of the chain in such a way that the resonance H^* will be directly created.

iii) For $m_H \leq M_{chain} \leq m_{H^*}$ we also correct the x-fractions in order to create directly the stable hadron H (pseudoscalar meson or spin ½ baryon).

iv) In the case of $M_{chain} < m_H$ we sample a new event. For diquark-antidiquark chains we always demand an invariant mass larger than 2.3 GeV/c^2 to be able to create a baryon and an antibaryon. Otherwise we sample a new event.

Our Monte Carlo chain-decay model conserves energy-momentum and quantum numbers for each chain exactly; therefore we obtain final hadron states conserving these quantities too.

Generating events in a hadron-nucleus interaction is more complicated since many collisions occur:

1) Define the kind of projectile P, target nucleus T, and the laboratory momentum p_0 of the projectile.

2) Sample the number ν of collisions during the interaction process using a Poisson distribution with an average ν-value given in Eq. (1). Taking the picture of multiple interaction inside the nucleus seriously one can from the density distribution inside the nucleus directly determine this multiplicity distribution [20], which turns out to be quite different from a Poisson distribution. We leave it to further work to study how much measurable cross-sections are influenced by the exact form of this multiplicity distribution.

3) Construct ν two-chain systems as in hadron-hadron collisions: one collision occurs between the valence quarks of the projectile and the valence quarks of a nucleon of the target nucleus. All other $\nu - 1$ collisions occur between quark-antiquark pairs of the parton sea of the projectile and the valence quarks of further target nucleons as in a meson-baryon collision.

4) Other than in hadron-hadron interactions we have to take into account not only the valence quarks but also the sea quarks of the projectile. The energy fractions x_P^{val} and x_T^{val} for the single valence quarks of projectile P and target T particles, respectively, are obtained from distributions (4) or (5). The fractions x_P^{sea} of the sea quarks of the projectile are sampled according to

$$d^{sea}(x) \approx \frac{(1-x)^4}{x} . \qquad (6)$$

The remaining valence diquarks of the target nucleons now carry the x-fraction $1 - x_T^{val}$, whereas the remaining quark or diquark of the projectile is given the x-fraction $1 - x_P^{val} - \sum_{sea} x_P^{sea}$. The sum is taken over all sea quarks which take part in the interaction. For kinematic reasons we neglect chains containing sea quarks which carry an energy of less than 2 GeV and we sample a complete new event if the energy of the two-chains containing only valence quarks is less than 4 GeV.

5) Going into the c.m.s. of each chain, we can hadronize the chains as in hadron-hadron collisions.

6) Adding all produced chains and hadrons in the laboratory frame, we obtain the whole final hadron state of the considered hadron-nucleus collision.

A description of the underlying Monte Carlo program will be given elsewhere [21].

5. RESULTS OF THE MODEL AND COMPARISON WITH DATA

We compare the results of our two-chain model for hadron-hadron collisions and of our multi-chain model for hadron-nucleus collisions with data [7,22-27]. We also present some Monte Carlo results of our multi-chain model concerning average particle multiplicities depending on the mass number A of the nucleus and the laboratory momentum.

At first we show results of our model for hadron-hadron collisions. Proton-proton interactions are especially well known experimentally. In Fig. 5 we plot average multiplicities for several charged particles versus the squared c.m. energy s of the pp collision and compare it with data from Ref. [22]. In general we find a reasonably good agreement with the data. For larger p_{lab} values we get average multiplicities for antiprotons, which are somewhat below the data. This may be due to the fact that we use probabilities appropriate to incoming diquarks in the emission of baryons or mesons (see Fig. 4). This has not yet been tested carefully enough in comparison with data.

In Figs. 6a to 6e we present also average multiplicities for $\pi^{\pm}$, $K^{\pm}$, π^0, $\bar{p}$, and $\Lambda(\bar{\Lambda})$. We find again a good agreement with data given in a compilation by Anisovich and Nyiri [24]. In the case of charged kaons (Fig. 6b) our Monte Carlo results might increase somewhat too fast compared to data, but experimental errors for $K^{\pm}$ production are not well known at the present time.

For $\bar{\Lambda}$ production (see Fig. 6e) we get a very nice agreement with the data given in Ref. [24], whereas the average multiplicities for Λ particles seem to be too large. Taking into account that the two data points of Ref. [24] above $s \approx 1000\ \mathrm{GeV}^2$ are only lower limits and using a more recent result from Ref. [23] in this energy region, we are also able to describe average Λ multiplicities reasonably well. A more detailed comparison of strange-particle production requires more accurate data.

In Fig. 7 we consider KNO multiplicity distributions for charged-particle production in pp collisions for laboratory momenta between 40 and 640 GeV/c. Since in our model diffractive events are not included, we get in the region for small charged multiplicities Monte Carlo results which are too low compared to data [25-27].

Looking for rapidity distributions we consider in Fig. 8 the rapidity

$$y = \frac{1}{2}\ln\left[\frac{E + p_L}{E - p_L}\right] = \ln\left[\frac{E + p_L}{\sqrt{p_T^2 + m^2}}\right] \tag{7}$$

as well as the pseudorapidity

$$\eta = -\ln\left[\mathrm{tg}\left(\frac{\theta_{lab}}{2}\right)\right] , \tag{8}$$

where θ_{lab}, E, and p_L are the laboratory quantities of polar angle, energy, and longitudinal momentum with respect to the beam axis. The results of our hadron-hadron Monte Carlo model for different laboratory momenta p_{lab} indicate that one has to be careful in using rapidity or pseudorapidity since the shapes differ significantly from one another. The reason is that our model does not only contain pions. A qualitative discussion shows that our model provides rapidity distributions with a more or less correct behaviour. This includes the increase of the height of the plateau as well as the broadening of the plateau with rising energy. Even quantitatively the height of the plateaux is in the right order of 2 found at ISR energies. Of course the absence of diffractive events in our model will mainly influence the behaviour of the left and the right tail of the rapidity distributions.

Now we present results of the hadron-nucleus Monte Carlo model and compare them with the data measured at the CERN SPS [7]. We first have to mention that these are results obtained without a careful optimization of several free parameters of our model. So we neglect chains with energies below some fixed lower limit (see Section 4). Taking the model more seriously one has to consider also the Fermi momentum of the nucleons of the target nucleus and one has to take into account diffractive events. We have not done this up to now. Neglecting the Fermi momentum of the nucleons would probably not allow the description of rapidity distributions for negative rapidities in detail.

In Fig. 9 average charged multiplicities are plotted versus the average number of collisions $\langle\nu\rangle$ inside the nucleus. The Monte Carlo results for proton-nucleus collisions at p_{lab} = 100 GeV/c are compared with data for different projectiles and energies. The multiplicities provided by our hadron-nucleus model are somewhat too low at small $\langle\nu\rangle$ values and increase faster with $\langle\nu\rangle$ than the data. On the other hand, looking for KNO distributions in pp collisions (see Fig. 7) we find that our curves at small multiplicities decrease faster than data. This indicates that our hadron-hadron two-chain model provides somewhat too high multiplicities on the average. On the other hand, our average multiplicities in the case of proton-nucleus collisions at $\langle\nu\rangle \approx 1$ are too low. Decreasing our multiplicities in pp collisions we would get even lower multiplicities in p-A collisions at small $\langle\nu\rangle$ values. It is not clear what one has to do in order to avoid this contradiction. Arguments explaining the faster increase of the average multiplicities at larger $\langle\nu\rangle$ in comparison with data are the following: In the case of data, grey prongs representing slow particles have been subtracted. We consider here all charged particles. Furthermore, we neglect very light chains. So probably we obtain larger multiplicities at higher $\langle\nu\rangle$. Eventually there might also be some differences in calculating the average number of collisions $\langle\nu\rangle$ compared to the procedure used in Ref. [7]. Nevertheless in this first approximation our results agree reasonably well with the data.

In Figs. 10a and b we present pseudorapidity distributions produced in π^--A collisions for different nuclei at p_{lab} = 37 GeV/c and for π^+-Cu collisions at several laboratory momenta. In both cases our model is in good agreement with the data.

Finally we show model predictions of our hadron-nucleus model for average multiplicities of all particles, all charged particles, and several kinds of neutral and charged particles at larger energies. In Fig. 11 the A-dependence at p_{lab} = = 400 GeV/c is presented and in Fig. 12 we plot the p_{lab}-dependence up to 2500 GeV/c at A = 100. In this figure we show also average multiplicities for all charged particles, protons, and neutrons, produced in pp collisions.

6. SUMMARY

We have developed a multi-chain model for hadron-nucleus collisions based on the dual parton model. The hadronization of quarks and diquarks is realized via a chain-decay fragmentation model. Our model includes quantum-number structure and correct kinematics. So we are able to calculate final hadronic states conserving energy momentum and quantum numbers exactly. The formulation on the basis of a Monte Carlo method allows the calculation of several inclusive distributions as well as the simulation of exclusive quantities. In this sense the model can be used as an event generator for hadron-hadron and hadron-nucleus interactions.

The model presented here is not in a final state. There are several possibilities in order to make it more realistic in future. So at present we have not included the Fermi momentum of the nucleons and we have not taken into account diffractive events. Furthermore, we did not really optimize several free parameters of the model, such as the energy-sharing function for baryons or the energy cut for light chains. Even without this optimization we are able to present results which agree reasonably well with data.

Acknowledgements

We wish to thank H.J. Möhring for discussions and for making available a model for hadron-nucleus cross-sections prior to publication. One of the authors (J.R.) acknowledges the contributions of K. Goebel and G.R. Stevenson to discussions and for the possibility of performing a large part of the work reported during a stay at CERN and K. Hänssgen and Sylvia Henger for running computer programmes.

REFERENCES

[1] T. DeGrand and H.F. Miettinen, Phys. Rev. Lett. 40, 612 (1978);
T. DeGrand, Phys. Rev. D 19, 1398 (1979);
J. Ranft, Phys. Rev. D 18, 1491 (1978);
J. Kalinowski, S. Pokorski and L. Van Hove, Z. Phys. C2, 85 (1979);
K.P. Das and R.C. Hwa, Phys. Lett. 68B, 459 (1977);
R.C. Hwa, Phys. Rev. D 22, 759 and 1593 (1980).

[2] W. Ochs, Nucl. Phys. B118, 397 (1977).

[3] B. Anderson, G. Gustafson and C. Peterson, Phys. Lett. 69B, 221 (1977); Phys. Lett. 71B, 337 (1977); Z. Phys. C1, 105 (1979).

[4] A. Capella, U. Sukhatme, C.I. Tan and J. Tran Thanh Van, Phys. Lett. 81B, 68 (1979);
A. Capella, U. Sukhatme and J. Tran Thanh Van, Z. Phys. C3, 329 (1980).

[5] A. Capella, Lecture at 16th Rencontre de Moriond, Les Arcs, 1981, Orsay, preprint LPTHE 81/15 (1981).

[6] J.D. Bjorken, Lecture at 2nd Int. Conf. on Physics in Collision, Stockholm, 1982, Fermilab preprint, Fermilab-Conf.82/42 THY (1982).

[7] M.A. Faessler, Ann. Phys. (NY) 137, 44 (1981).

[8] A. Białas, W. Czyz and W. Furmanski, Acta Phys. Pol. B8, 585 (1977);
V.V. Anisovich, Yu.M. Shabelski and V.M. Shekhter, Nucl. Phys. B133, 477 (1978);
N.N. Nikolaev, Fiz. Elem. Chastits At. Yadra 12, 162 (1981).

[9] C.B. Chiu and D.M. Tow, Phys. Lett. 97B, 443 (1980);
W.Q. Chao et al., Phys. Rev. Lett. 44, 578 (1980).

[10] A. Capella and J. Tran Thanh Van, Phys. Lett. 93B, 146 (1980) and Z. Phys. C10, 249 (1981).

[11] W. Kittel, review given at the 12th Int. Symposium on Multiparticle Dynamics, Notre Dame, 1981, Nijmegen preprint HEN 212 (1981).

[12] S. Ritter and J. Ranft, Acta Phys. Pol. B11, 259 (1980).

[13] S. Ritter, Leipzig preprint KMU-HEP 82-03 (1982), to be published in Z. Phys. C.

[14] S. Ritter, Description of the Monte Carlo code BAMJET, to be published in Computer Physics Communications (1983).

[15] S. Ritter, unpublished.

[16] P. Aurenche, F.W. Bopp and J. Ranft, unpublished.

[17] V.A. Abramovski, V.N. Gribov and O.V. Kancheli, Yad. Fiz. 18, 595 (1971).

[18] A. Capella and J. Tran Thanh Van, Orsay preprint LPTHE 82/12 (1982);
P. Aurenche and F.W. Bopp, Phys. Lett. 114B, 363 (1982), Z. Phys. C13, 205 (1982);
A.B. Kaidalov and K.A. Ter-Martyrosian, ITEP preprint ITEF-51 (1982);
A.B. Kaidalov, ITEP preprint ITEF-50 (1982).

[19] J. Wetzig, K. Hänssgen, R. Kirschner, J. Ranft and S. Ritter, Leipzig preprint KMU-HEP 79-14 (1979);
K. Hänssgen and S. Ritter, Description of the code Decay, to be published in Computer Physics Communications (1983).

[20] G. Nilsson and E. Stenlund, Lund University preprint LU-TP 80-9 (1980).

[21] J. Ranft and S. Ritter, Description of the Monte Carlo codes NUCEVT and HADEVT, internal report CERN TIS/RP/IR/83-23 (1983).

[22] M. Antinucci et al., Lett. Nuovo Cimento 6, 121 (1973).

[23] D. Drijard et al., Z. Phys. C12, 217 (1982).

[24] V.V. Anisovich and J. Nyiri, Budapest preprint KFKI-1981-56 (1981).

[25] V.V. Ammosov et al., Nucl. Phys. B58, 77 (1973).

[26] S. Barish et al., Phys. Rev. D 9, 2689 (1974).

[27] A. Firestone et al., Phys. Rev. D 10, 2080 (1974).

Figure captions

Fig. 1 : All possible diagrams for two-chain systems in (a) baryon-baryon, (b) antibaryon-baryon, and (c) meson-baryon interactions. B, $\bar{B}$, M stand for baryon, antibaryon and meson; and x^q and x^d are the quark and diquark momentum fractions, respectively. The indices P and T stand for projectile and target particle, respectively.

Fig. 2 : Example of a triple-scattering diagram in a proton-nucleus interaction. P represents the incoming proton and T_1, T_2, and T_3 are the three target nucleons taking part in the interaction. x^v and x^{S_i} are valence and sea-quark momentum fractions.

Fig. 3 : Typical two-jet systems for an incident

(a) quark and diquark,

(b) diquark and antidiquark.

q, qq and $\overline{qq}$ stand for quark, diquark and antidiquark; and M, B, and $\bar{B}$ stand for meson, baryon, and antibaryon, respectively.

Fig. 4 : All possible vertices during the chain decay of an incoming quark q (antiquark $\bar{q}$) or diquark qq (antidiquark $\overline{qq}$) and their probabilities. M, B and $\bar{B}$ stand for meson, baryon, and antibaryon, respectively.

Fig. 5 : Average multiplicities for all charged particles, $\pi^{\pm}$, $K^{\pm}$, p, and $\bar{p}$, produced in pp collisions as a function of the squared c.m. energy s. The results of our Monte Carlo model for hadron-hadron interactions are compared with data from Ref. [22].

Fig. 6 : Average multiplicities for

(a) charged pions $\pi^{\pm}$,

(b) charged kaons $K^{\pm}$,

(c) neutral pions π^0,

(d) antiprotons $\bar{p}$,

(e) lambdas and antilambdas Λ, $\bar{\Lambda}$

produced in pp collisions. The data [23,24] are compared with results of our hadron-hadron Monte Carlo model.

Fig. 7 : KNO multiplicity distributions for charged particles in the laboratory momentum range p_{lab} = 40 GeV/c to 640 GeV/c. The results of our Monte Carlo model are compared with the data [25,26,27] from pp collisions.

Fig. 8 : Pseudorapidity distributions $dN/d\eta$ and rapidity distributions dN/dy for several laboratory momenta p_{lab} in pp collisions provided by our hadron-hadron Monte Carlo model.

Fig. 9 : Average charged multiplicity $\langle n_{ch} \rangle$ versus the average number of collisions $\langle \nu \rangle$. The results of our hadron-nucleus Monte Carlo model for proton-nucleus interactions at p_{lab} = 100 GeV are compared with data [7] for different projectiles and energies. The lines are drawn to guide the eye.

Fig. 10 : Pseudorapidity distributions $dN/d\eta$ for
(a) π^- projectile and different target nuclei at p_{lab} = 37 GeV/c,
(b) π^+ projectile and different p_{lab} for a copper target (A = 63).
The results of the hadron-nucleus Monte Carlo model, represented by histograms, are compared with data [7].

Fig. 11 : Predictions of the hadron-nucleus Monte Carlo model for average multiplicities for different charged and neutral particles versus the mass number A of the nucleus at p_{lab} = 400 GeV/c.

Fig. 12 : Predictions of the hadron-nucleus Monte Carlo model for average multiplicities for different charged and neutral particles versus the laboratory momentum p_{lab} at A = 100. In the case of average charged multiplicities and inclusive proton and neutron production, we also show results of our hadron-hadron Monte Carlo model for pp interactions at the same energy.

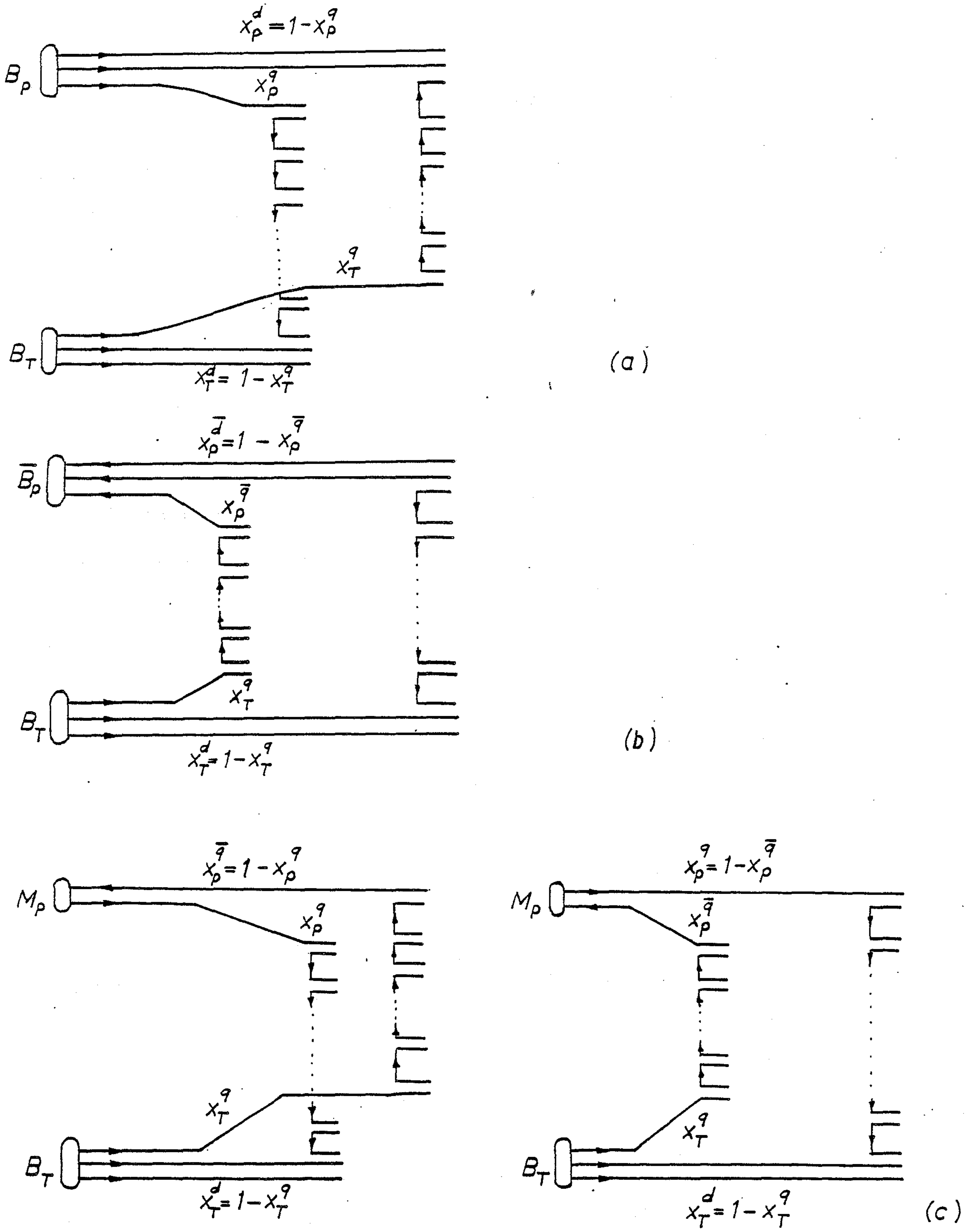
$x_P^d = 1 - x_P^q$
B_P
x_P^q
x_T^q
B_T
$x_T^d = 1 - x_T^q$
(a)
$x_P^{\bar{d}} = 1 - x_P^{\bar{q}}$
$\bar{B}_P$
$x_P^{\bar{q}}$
x_T^q
B_T
$x_T^d = 1 - x_T^q$
(b)
$x_P^{\bar{q}} = 1 - x_P^q$
M_P
x_P^q
x_T^q
B_T
$x_T^d = 1 - x_T^q$
$x_P^q = 1 - x_P^{\bar{q}}$
M_P
$x_P^{\bar{q}}$
x_T^q
B_T
$x_T^d = 1 - x_T^q$
(c)

Fig. 1

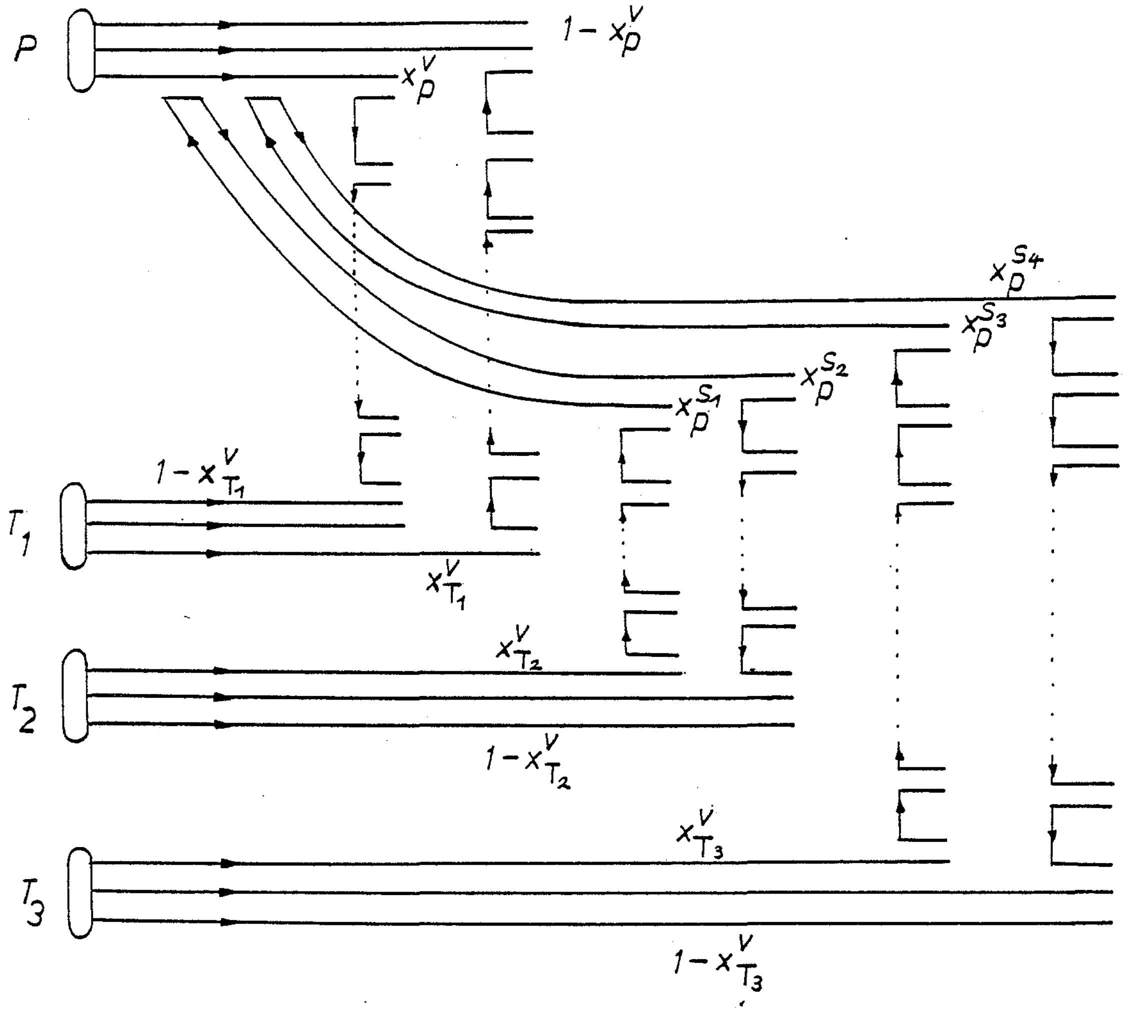

P
$1-x_P^V$
x_P^V
$x_P^{S_4}$
$x_P^{S_3}$
$x_P^{S_2}$
$x_P^{S_1}$
T_1
$1-x_{T_1}^V$
$x_{T_1}^V$
T_2
$x_{T_2}^V$
$1-x_{T_2}^V$
T_3
$x_{T_3}^V$
$1-x_{T_3}^V$

Fig. 2

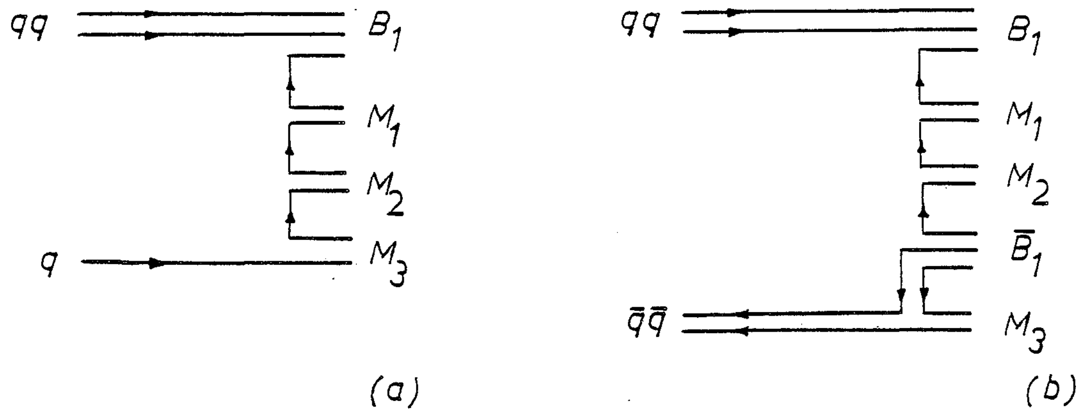

Fig. 3

vertex number IV	vertex	probability
1 (6)		0.95
2 (7)	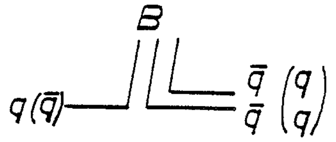	0.05
3 (8)	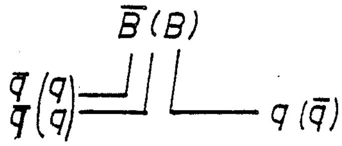	0.8
4 (9)		0.1
5 (10)	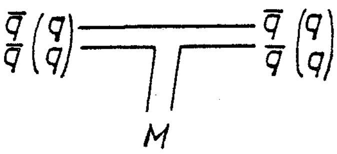	0.1

Fig. 4

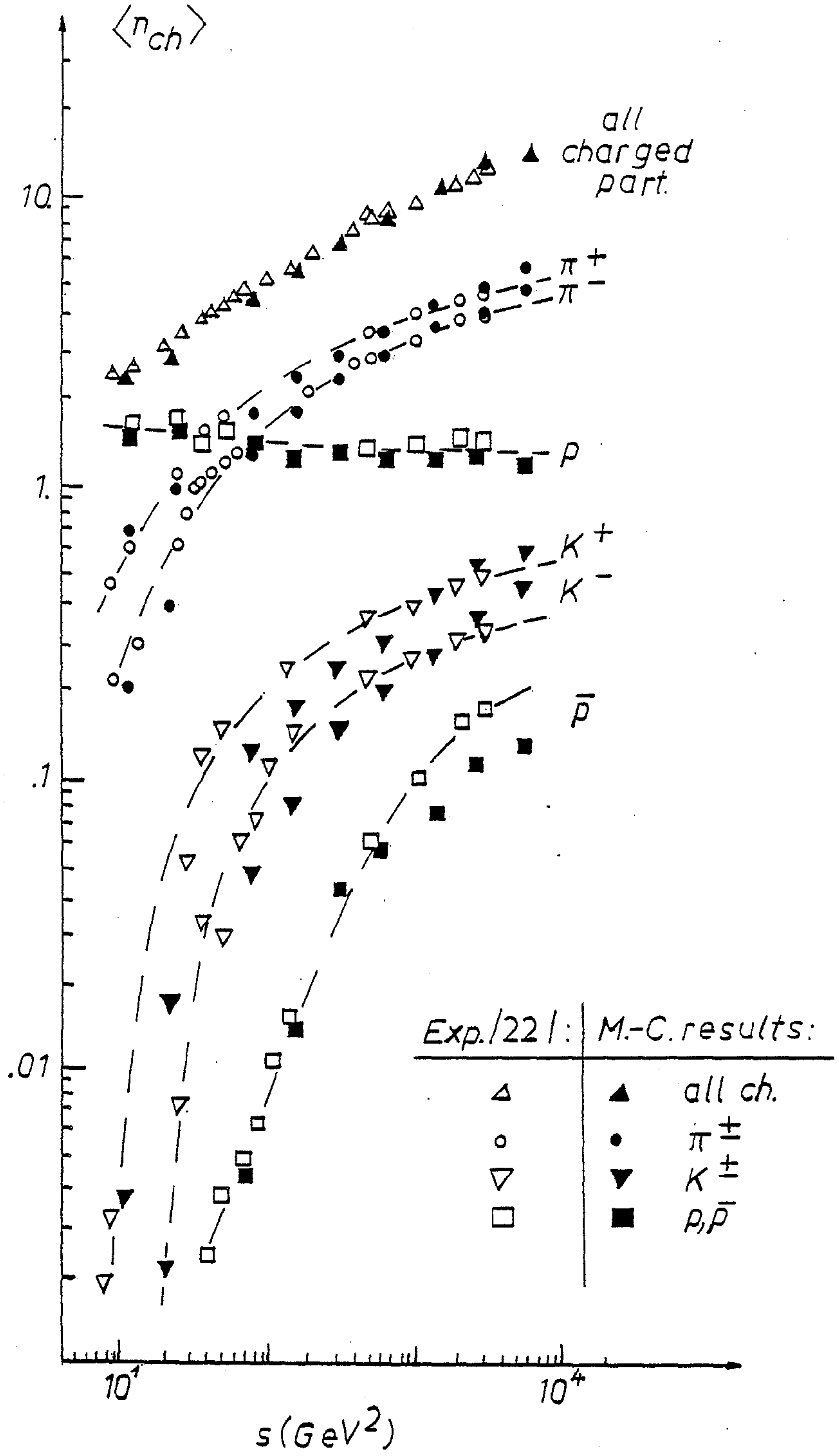
⟨n_ch⟩
all charged part.
π+
π−
p
K+
K−
p̄
10.
1.
.1
.01
10¹
10⁴
s (GeV²)
Exp./22/:
M.-C. results:
all ch.
π±
K±
p,p̄

Fig. 5

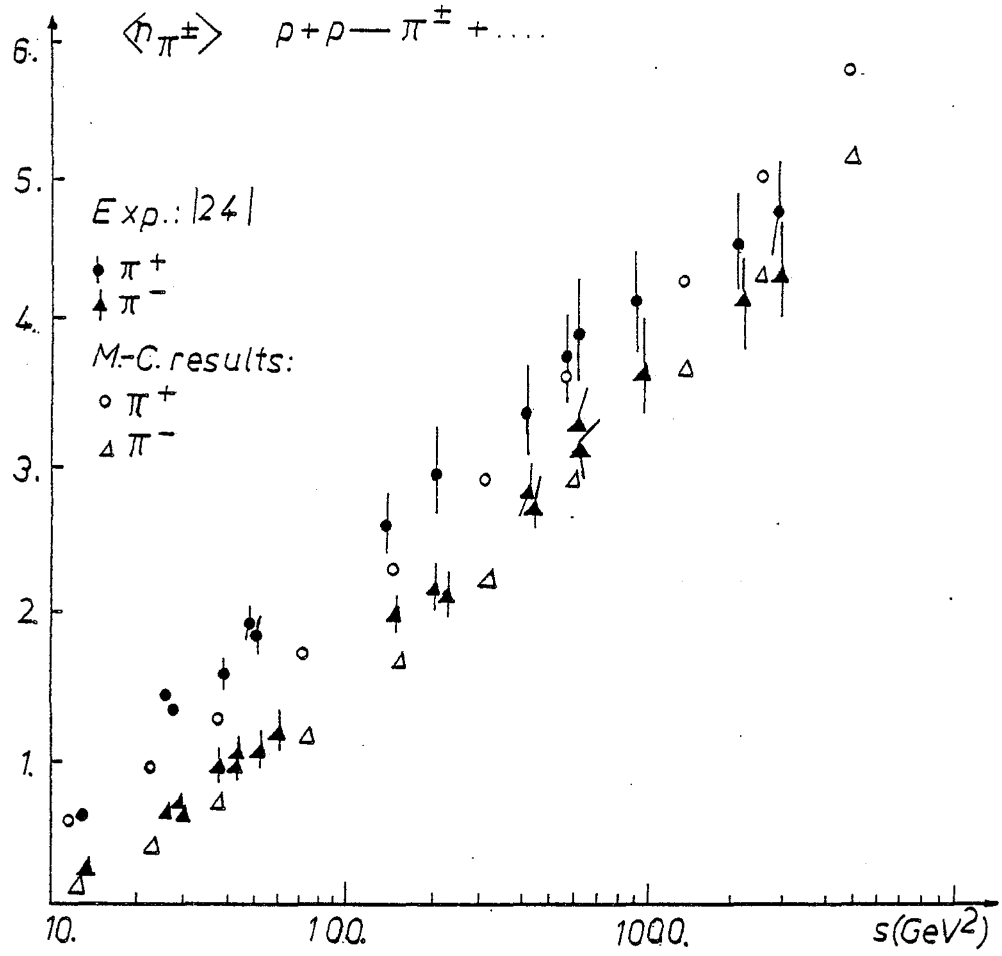

⟨n_π±⟩ p+p — π± + ...
Exp.: |24|
π+
π−
M.-C. results:
π+
π−
6.
5.
4.
3.
2.
1.
10.
100.
1000.
s(GeV2)

Fig. 6a

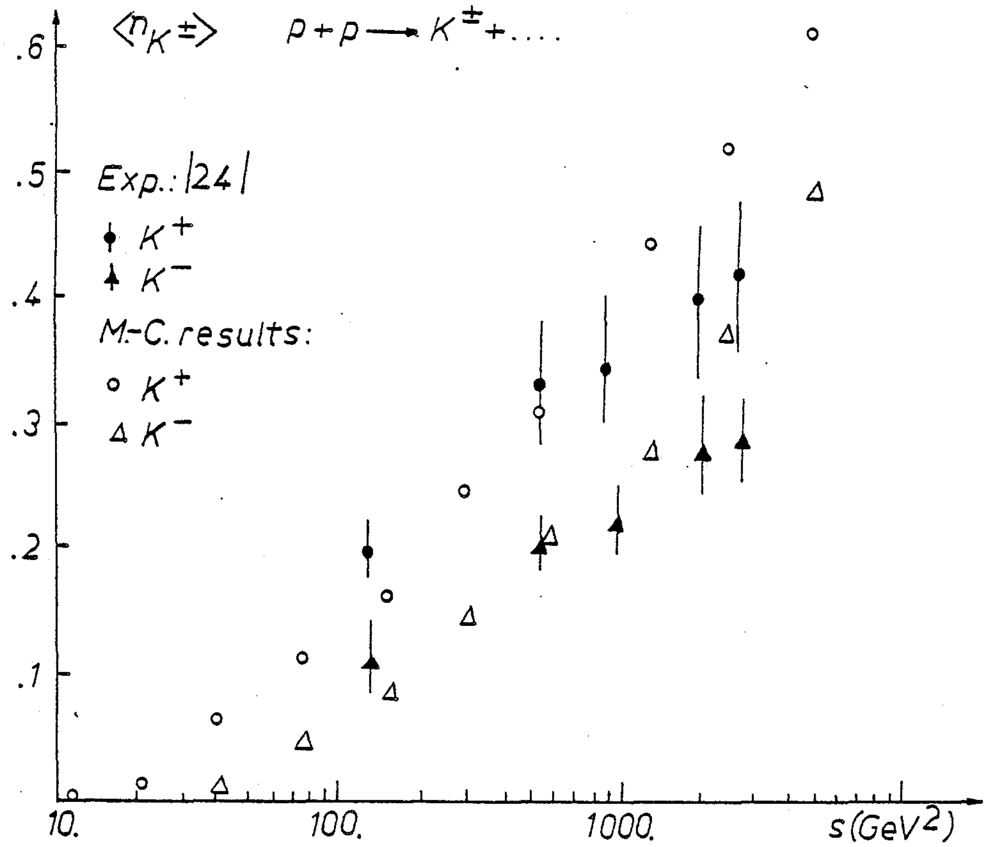

⟨n_K±⟩ p+p → K± + ...
Exp.: |24|
K+
K−
M.-C. results:
K+
K−
.6
.5
.4
.3
.2
.1
10.
100.
1000.
s(GeV2)

Fig. 6b

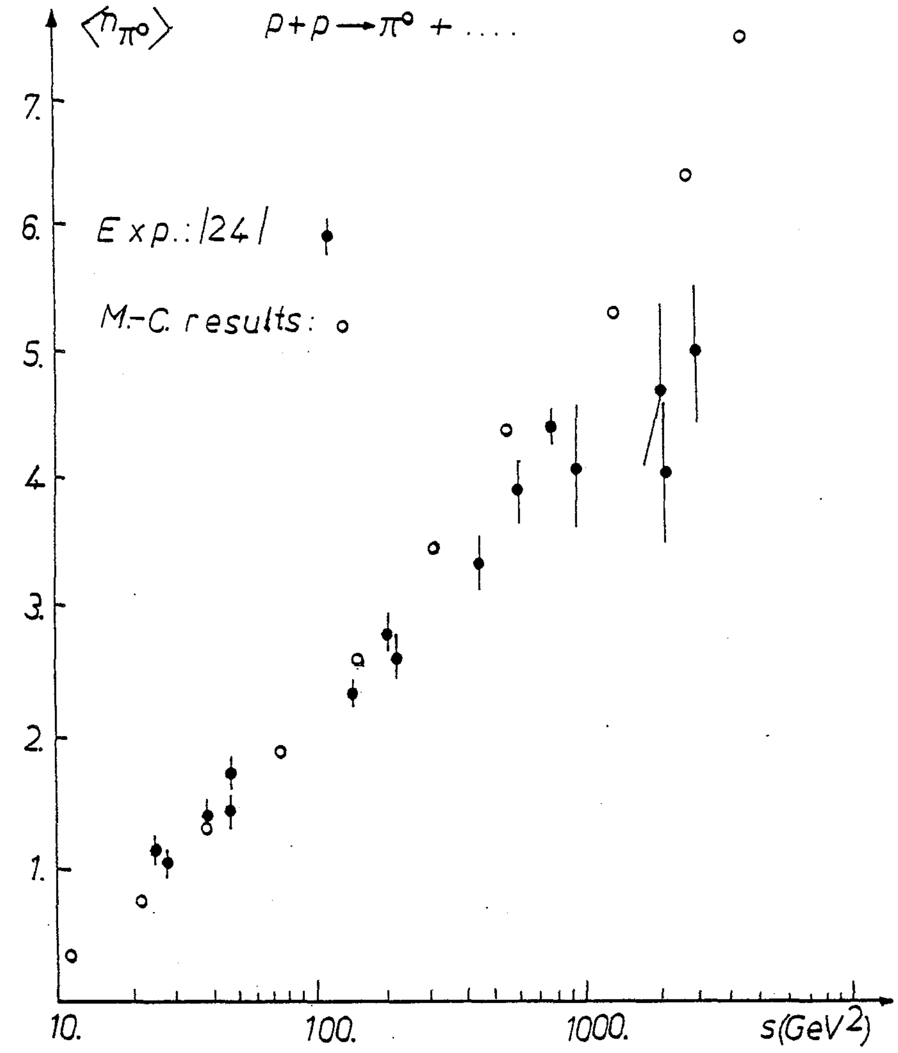

⟨n_π°⟩
p+p → π° + ...
7.
6.
5.
4.
3.
2.
1.
Exp.: /24/
M.-C. results:
10.
100.
1000.
s(GeV²)

Fig. 6c

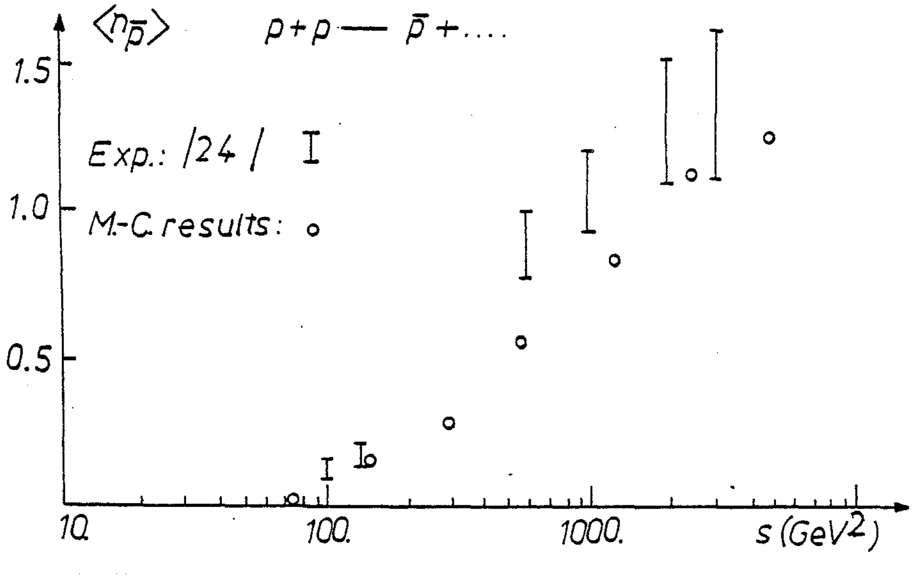

⟨n_p̄⟩
p+p — p̄ +....
1.5
1.0
0.5
Exp.: /24/
M.-C. results:
10.
100.
1000.
s (GeV²)

Fig. 6d

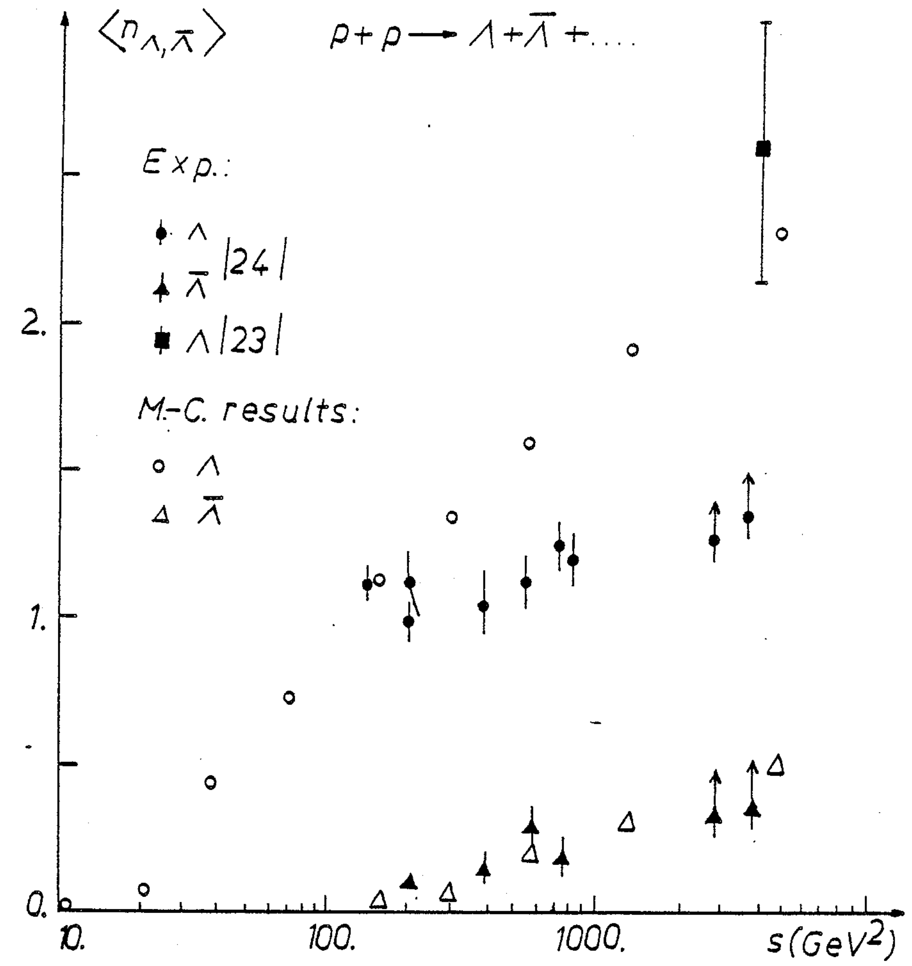

Fig. 6e

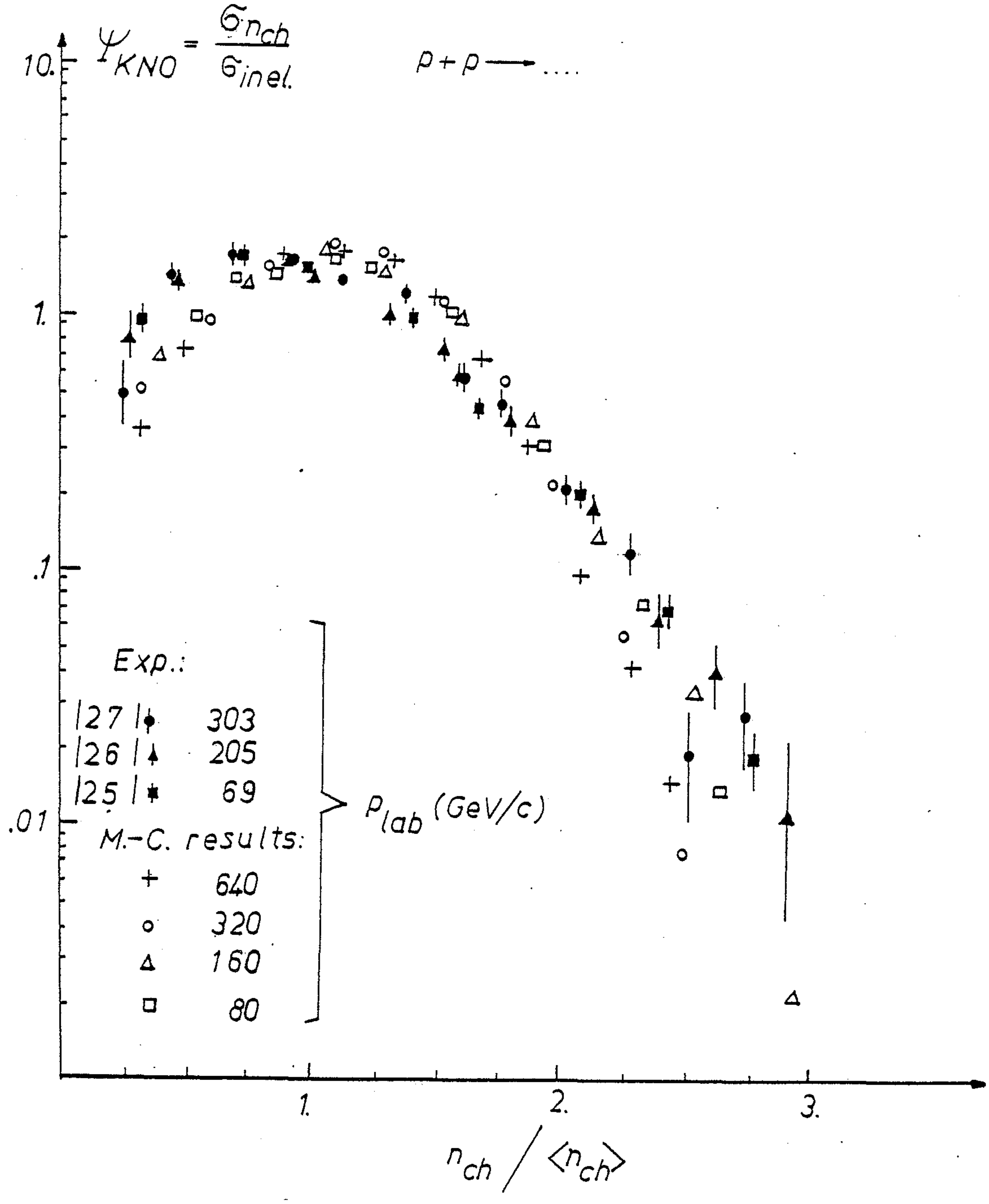
$\Psi_{KNO} = \frac{\sigma_{n_{ch}}}{\sigma_{inel.}}$
p + p ⟶ ....
10.
1.
.1
.01
Exp.:
|27| ● 303
|26| ▲ 205
|25| ■ 69
M.-C. results:
+ 640
○ 320
△ 160
□ 80
p_{lab} (GeV/c)
1.
2.
3.
$n_{ch} / \langle n_{ch} \rangle$

Fig. 7

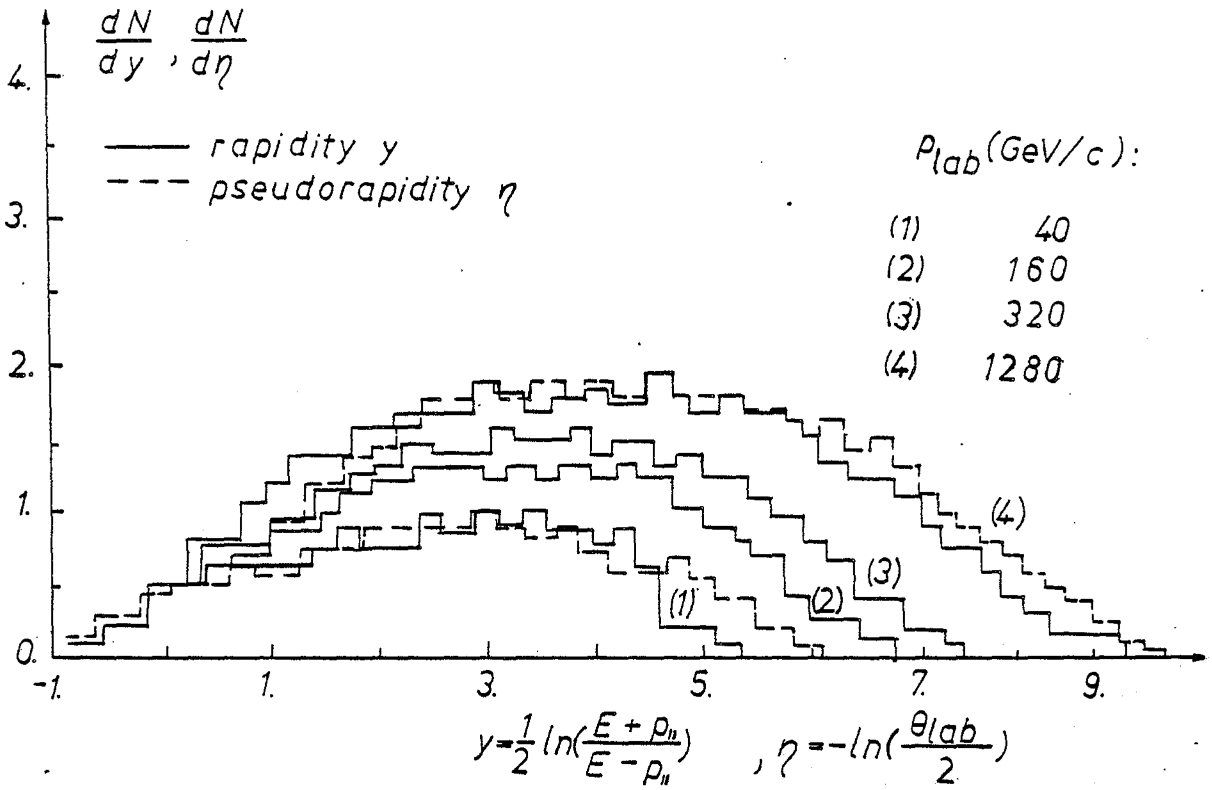

$\frac{dN}{dy}$, $\frac{dN}{d\eta}$
rapidity y
pseudorapidity η
p_{lab}(GeV/c):
(1) 40
(2) 160
(3) 320
(4) 1280
(1)
(2)
(3)
(4)
4.
3.
2.
1.
0.
-1.
1.
3.
5.
7.
9.
$y = \frac{1}{2} ln(\frac{E + p_{\parallel}}{E - p_{\parallel}})$, $\eta = -ln(\frac{\theta_{lab}}{2})$

Fig. 8

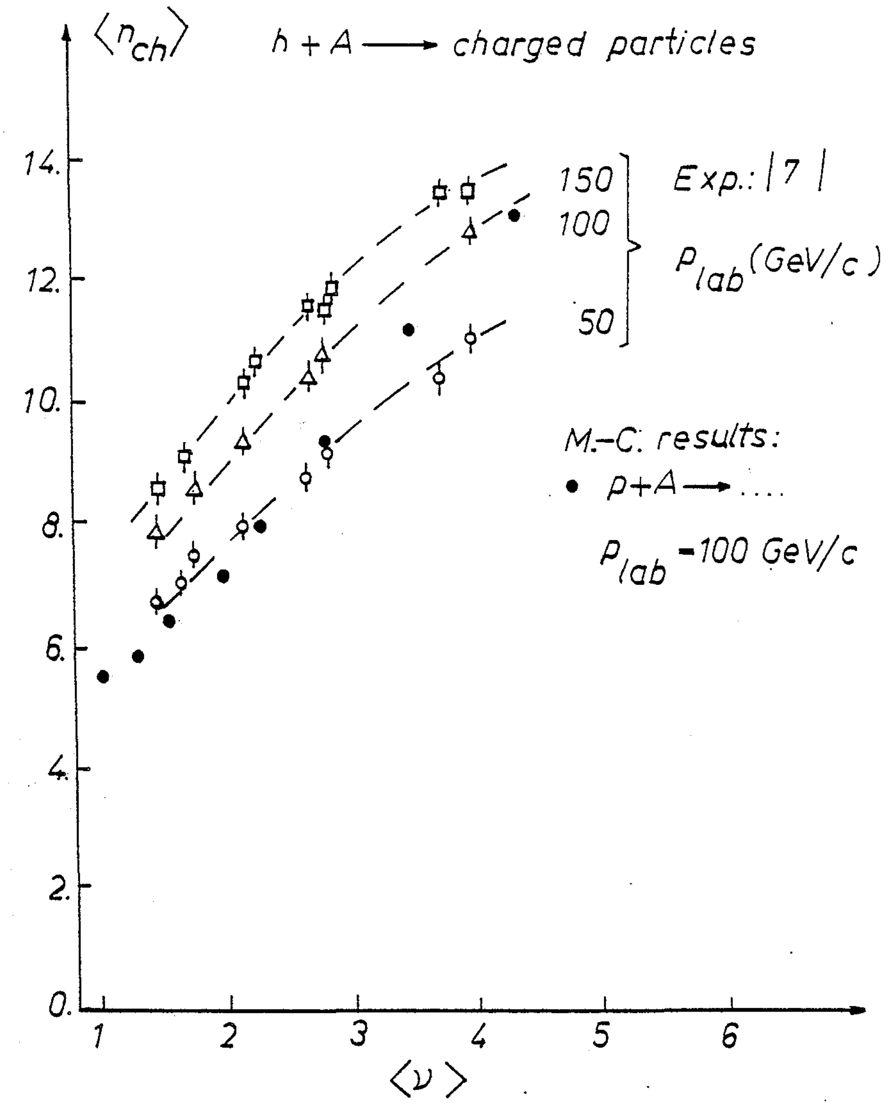

⟨n_ch⟩
h + A ⟶ charged particles
14.
12.
10.
8.
6.
4.
2.
0.
1
2
3
4
5
6
⟨ν⟩
150
100
50
Exp.: |7|
p_lab (GeV/c)
M.-C. results:
• p+A ⟶ ....
p_lab =100 GeV/c

Fig. 9

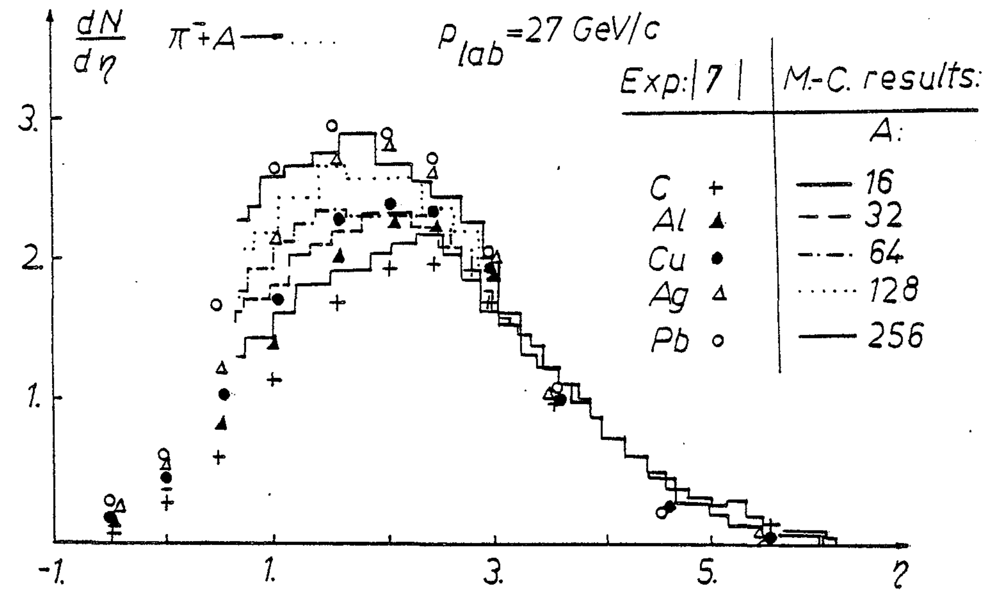

Fig. 10a

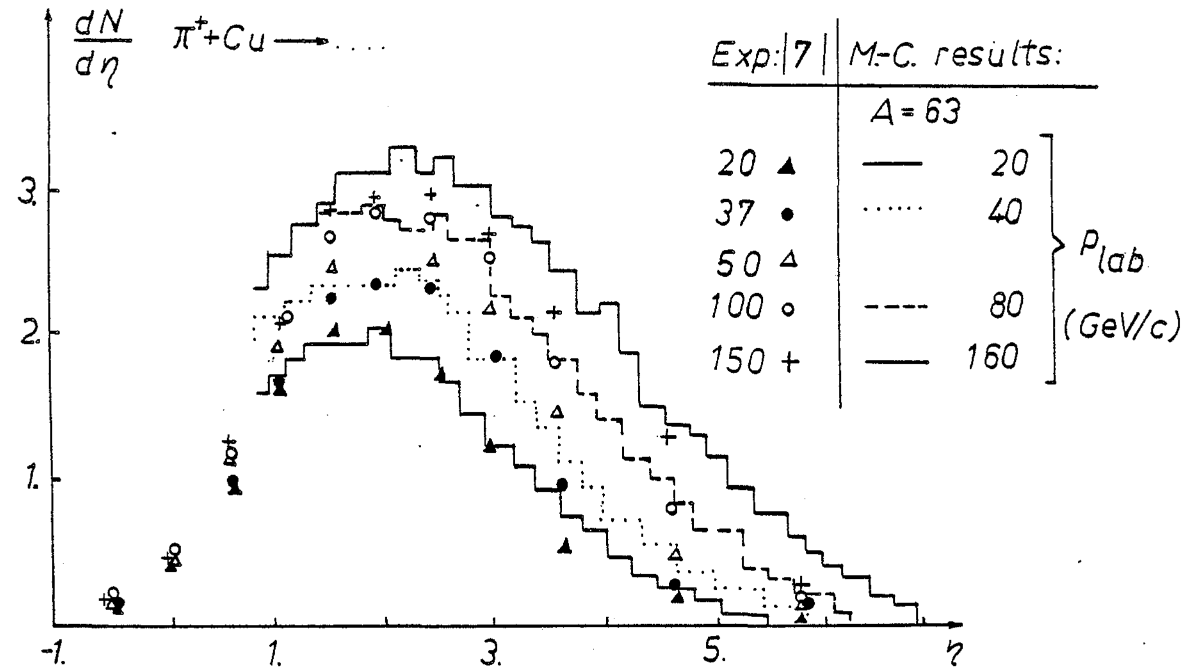

Fig. 10b

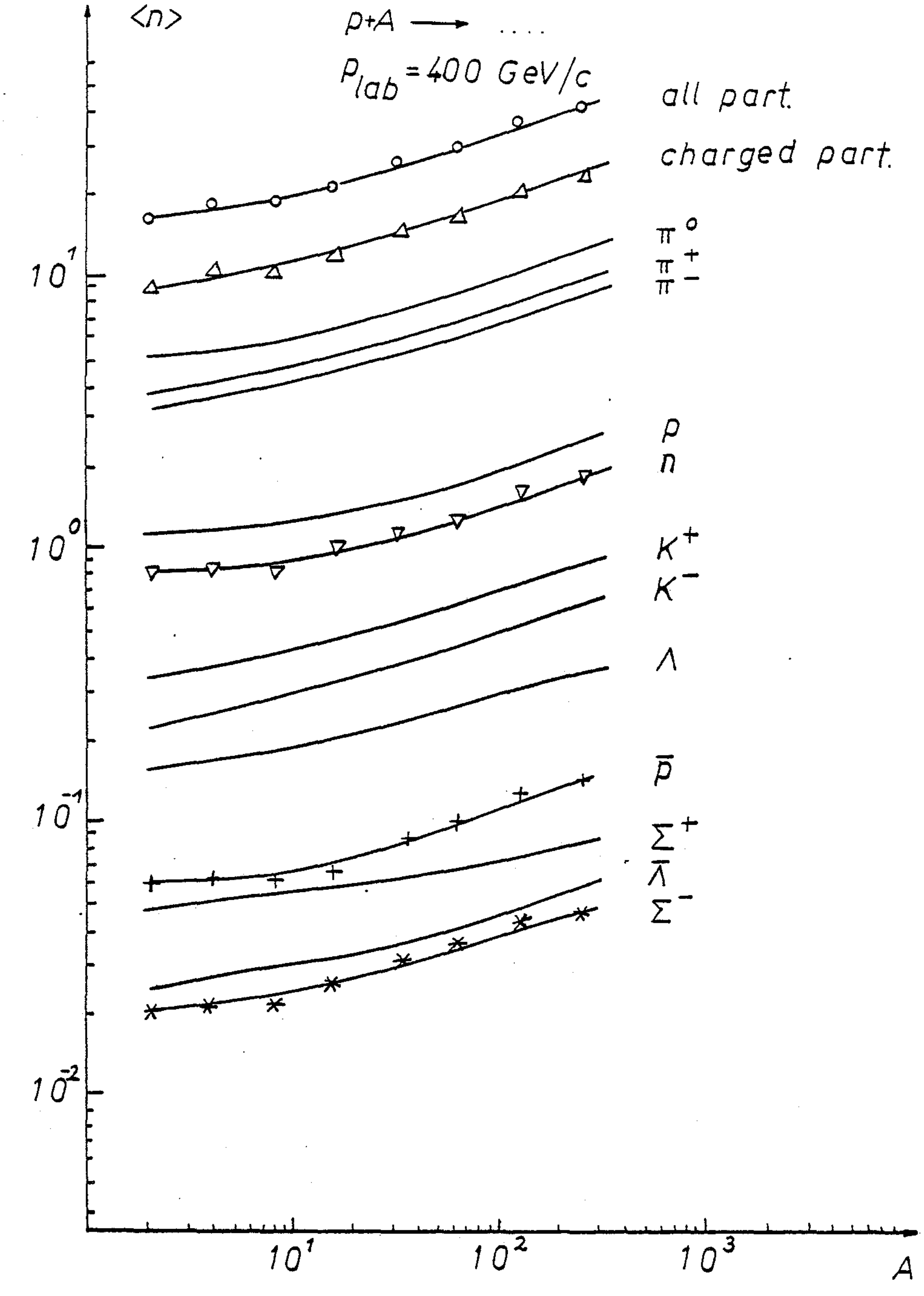

<n>
p+A ⟶ ....
p_lab = 400 GeV/c
all part.
charged part.
π°
π+
π−
p
n
K+
K−
Λ
p̄
Σ+
Λ̄
Σ−
10^1
10^0
10^-1
10^-2
10^1
10^2
10^3
A

Fig. 11

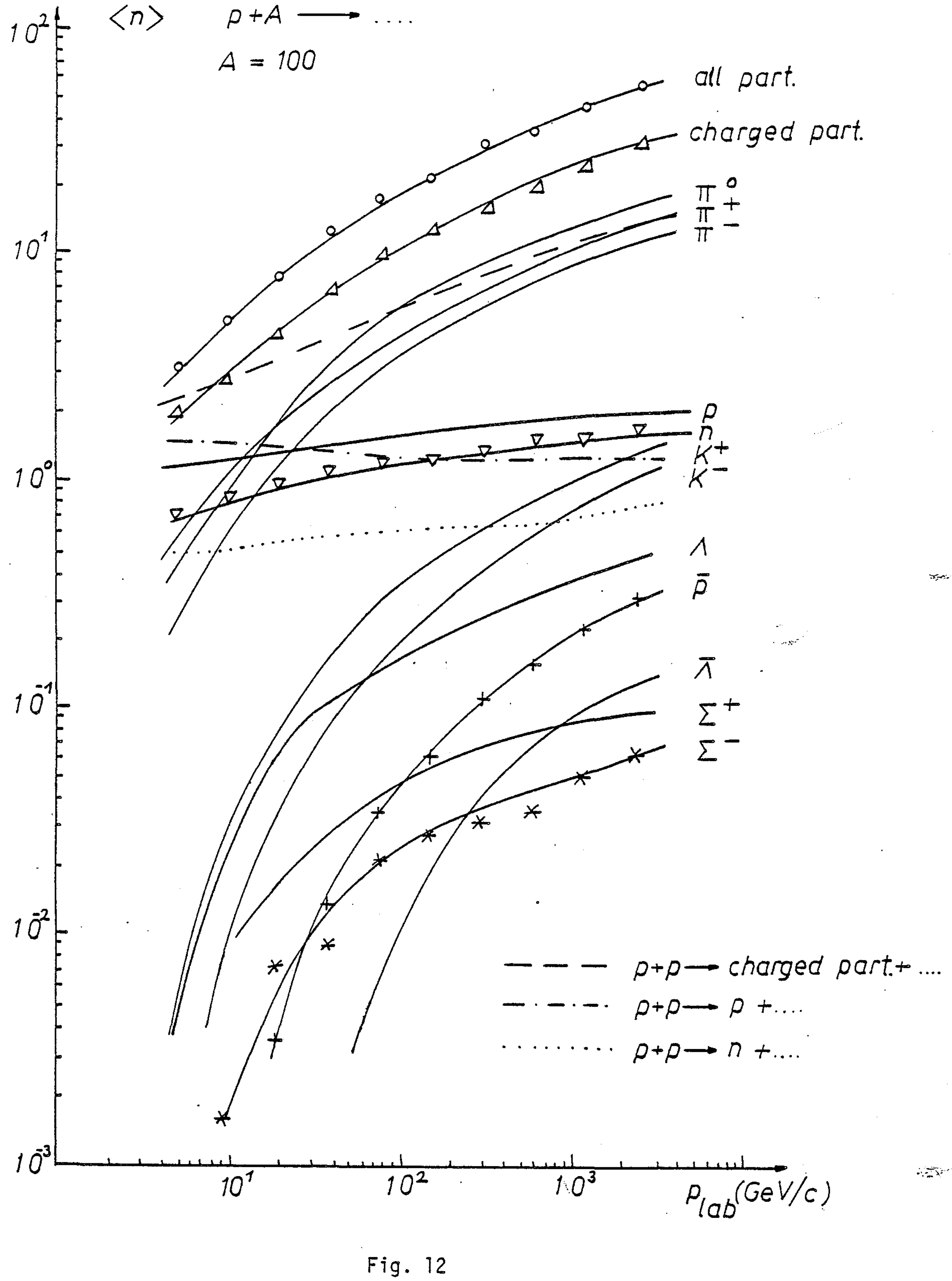

⟨n⟩
p + A ⟶ ....
A = 100
all part.
charged part.
π°
π⁺
π⁻
p
n
K⁺
K⁻
Λ
p̄
Λ̄
Σ⁺
Σ⁻
p+p ⟶ charged part.+ ....
p+p ⟶ p + ...
p+p ⟶ n + ...
P_lab (GeV/c)

Fig. 12